Supporting material for:

Ratiometric Array of Conjugated Polymers-Fluorescent Protein Provides a Robust Mammalian Cell Sensor

Subinoy Rana,[1,2,*] S. Gokhan Elci,[1] Rubul Mout,[1] Arvind K. Singla,[3] Mahdieh Yazdani,[1] Markus Bender,[4] Avinash Bajaj,[1,5] Krishnendu Saha,[1] Uwe H. F. Bunz,[4] Frank R. Jirik,[3] and Vincent M. Rotello[1,*]

[1]Department of Chemistry, University of Massachusetts Amherst, 710 North Pleasant Street, Amherst, MA 01003, USA. [2]Department of Materials, Imperial College London, Prince Consort Road, London SW7 2AZ, United Kingdom. [3]Department of Biochemistry and Molecular Biology, The McCaig Institute for Bone and Joint Health, Arnie Charbonneau Cancer Institute, University of Calgary, Calgary, Alberta, Canada. [4]Organisch-Chemisches Institut, Ruprecht-Karls-Universität Heidelberg, Im Neuenheimer Feld 270, 69120 Heidelberg, FRG. [5]Laboratory of Nanotechnology and Chemical Biology, Regional Centre for Biotechnology, 180 Udyog Vihar, Phase I, Gurgaon-122016, Haryana, India.

Table of Contents

S1. Materials

All chemicals and solvents for syntheses were purchased from Fisher Scientific and Sigma-Aldrich, and used without further purification, unless otherwise stated. CDβGeo, pTD and V14 cell lines were developed and donated by Prof. D. J. Jerry. The NT2/D1 cell line was donated by Prof. R. T. Zoeller. The three Sublines with organ-specific metastatic signatures were developed as described in the following sections. All other cell lines were purchased from American Type Culture Collection (ATCC) and were maintained according to the recommended guidelines. Five to six week old athymic (*nu*/*nu*), beige (NIH-III) female mice were purchased from Charles River Laboratories (St-Constant, QC). Mice were housed in viral antibody-free conditions in the University of Calgary Animal Resources Center. All experiments were conducted in compliance with Canadian Council of Animal Care guidelines and with ethical approval from the University of Calgary Animal Care Committee.

S2. Synthesis of polymers

Polymer **P1** and **P5** were synthesized as described in earlier reports.[1,2,3] **P2**, **P3** and **P4** polymers were synthesized from previously reported precursors[4,5] and prepared through reaction with iodomethane.[6]

Table S1. Structural parameters of the polymers used in the present study.

Polymers	M_n	M_w	PDI	n
P1	5,023	10,246	2.01	12
P2	10,840	21,029	1.90	15
P3	49,503	103,956	2.10	40
P4	9,445	23,335	1.26	9
P5	3,500	6,600	1.88	12

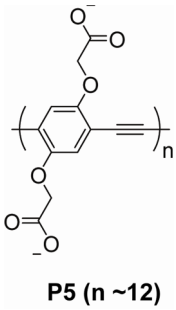

P5 (n ~12)

Figure S1. Structure of polymer **P5**, the anionic polymer used as the negative control.

S3. Expression of GFP

Starter cultures from a glycerol stock of GFP [enhanced GFP (eGFP) cloned into the pET21d vector (Novagen) where 6-His tag was located at *N*-terminal] in BL21(DE3) *E. coli* host was grown overnight in 50 mL of 2× YT media with 50 µL of 1000× ampicillin (16 g tryptone, 10 g yeast extract, 5 g NaCl in 1 L water). The cultures were shaken overnight at 250 rpm at 37 °C. The following day, 10 mL of the culture were inoculated in 1 L of 2× YT containing 1 mL 1000× ampicillin and shaken until $OD_{600} = 0.7$ was reached. This culture was then induced by adding isopropyl-β-D-thiogalactopyranoside (IPTG; 1 mM) and shaken at 28 °C. After 3 h, the cells were harvested by centrifugation (5000 rpm for 15 min) and lyzed in lysis buffer (2 mM imidazole, 50 mM NaH_2PO_4, 0.3 M NaCl) using a microfluidizer. Once lyzed, the solution was centrifuged at 15,000 rpm for 45 min at 4 °C. The supernatant was further purified using HisPur Cobalt-NTA columns (Pierce, cat. # 89969). The imidazole was removed by dialyzing in 5 mM sodium phosphate buffer (pH = 7.4). The purity of the protein was verified by gel electrophoresis, absorption and emission spectra.

S4. DLS and zeta-potential of the polymers and GFP

The hydrodynamic diameter and zeta potential of the CPs and GFP were measured in 5 mM phosphate buffer (pH=7.4) using Malvern ZetasizerNano ZS instrument. Each experiment was repeated three times and the average ± SD values are presented in the table below.

Table S2. Size and net charge of the polymers and GFP

Polymer/protein	Size (nm)	Zeta potential (mV)
P1	164 ± 3	+(6.5 ± 1)
P2	183 ± 16	+(7.1 ± 0.8)
P3	310 ± 32	+(8.0 ± 0.9)
P4	245 ± 13	+(5.9 ± 1.1)
P5	253 ± 9	-(16.0 ± 1.9)
GFP	10 ± 2	-(7.5 ± 1.1)

S5. Absorption and emission spectra of the CPs and GFP

Absorbance spectra were measured in a spectrophotometer. Emission spectra were recorded in Molecular Devices Spectramax M5 plate reader at an excitation of 430 nm.

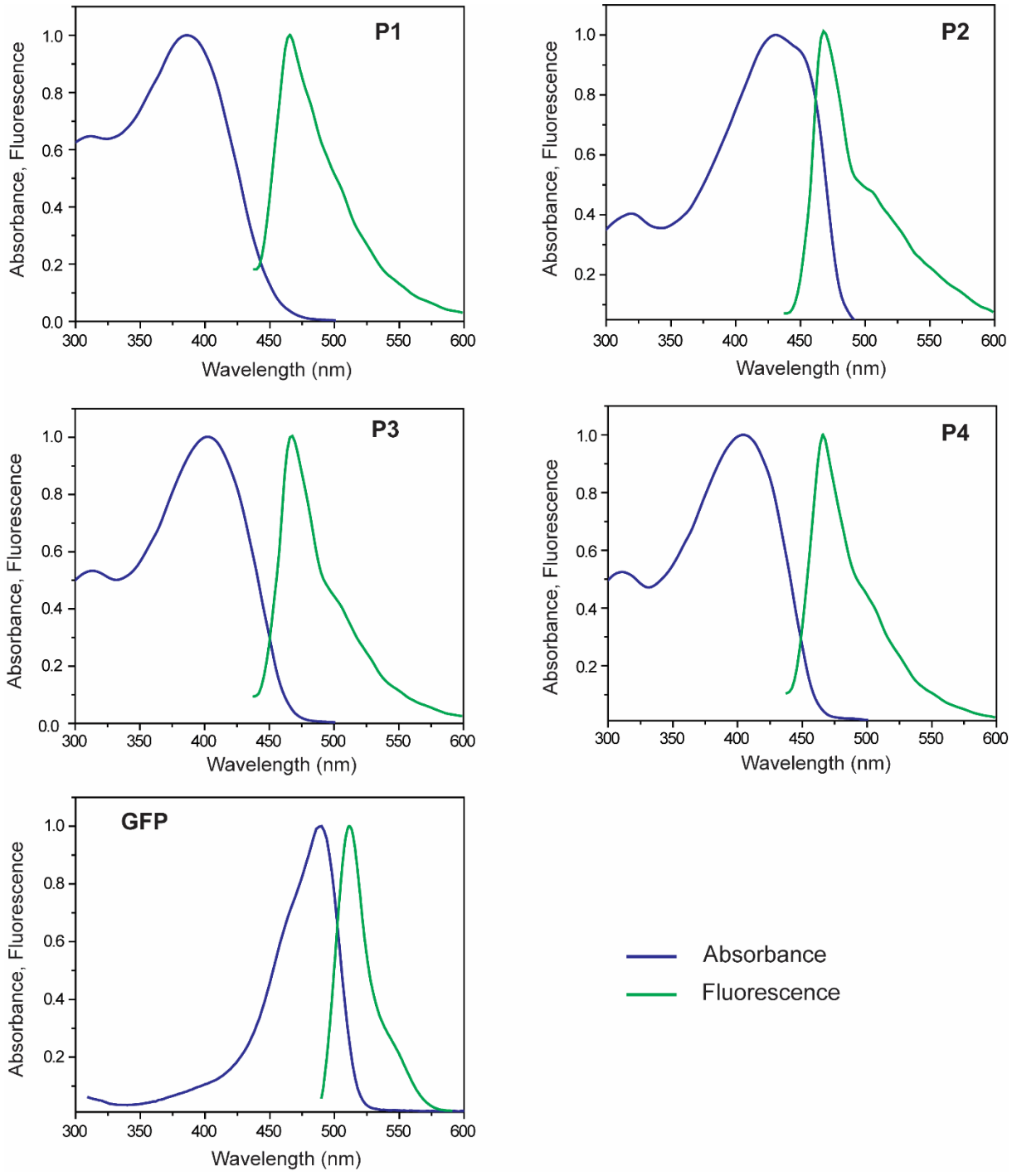

Figure S2. Normalized absorption and emission spectra of the CPs and GFP in 5 mM sodium phosphate buffer (pH 7.4).

S6. Fluorescence titrations of polymers with GFP

Fluorescence titration of the CPs (**P1-P5**) with GFP were carried out in a Molecular Devices Spectramax M5 plate reader. Different concentration of GFP was incubated with the CPs in black 96-well microplates (Costar) for 30 minutes at room temperature followed by recording the fluorescence spectra with an excitation wavelength of 430 nm. A cut-off of 455 nm was applied. The final concentration of GFP was 200 nM and that of **P1-P5** were between 8 to 300 nM. For the energy transfer studies, optimal concentrations of polymer and GFP complexes selected were **P1**: 300 nM, **P2**: 150 nM, **P3**: 8 nM, **NP4**: 50 nM (based on their molecular weights). We used **P5** (100 nM) as the negative control.

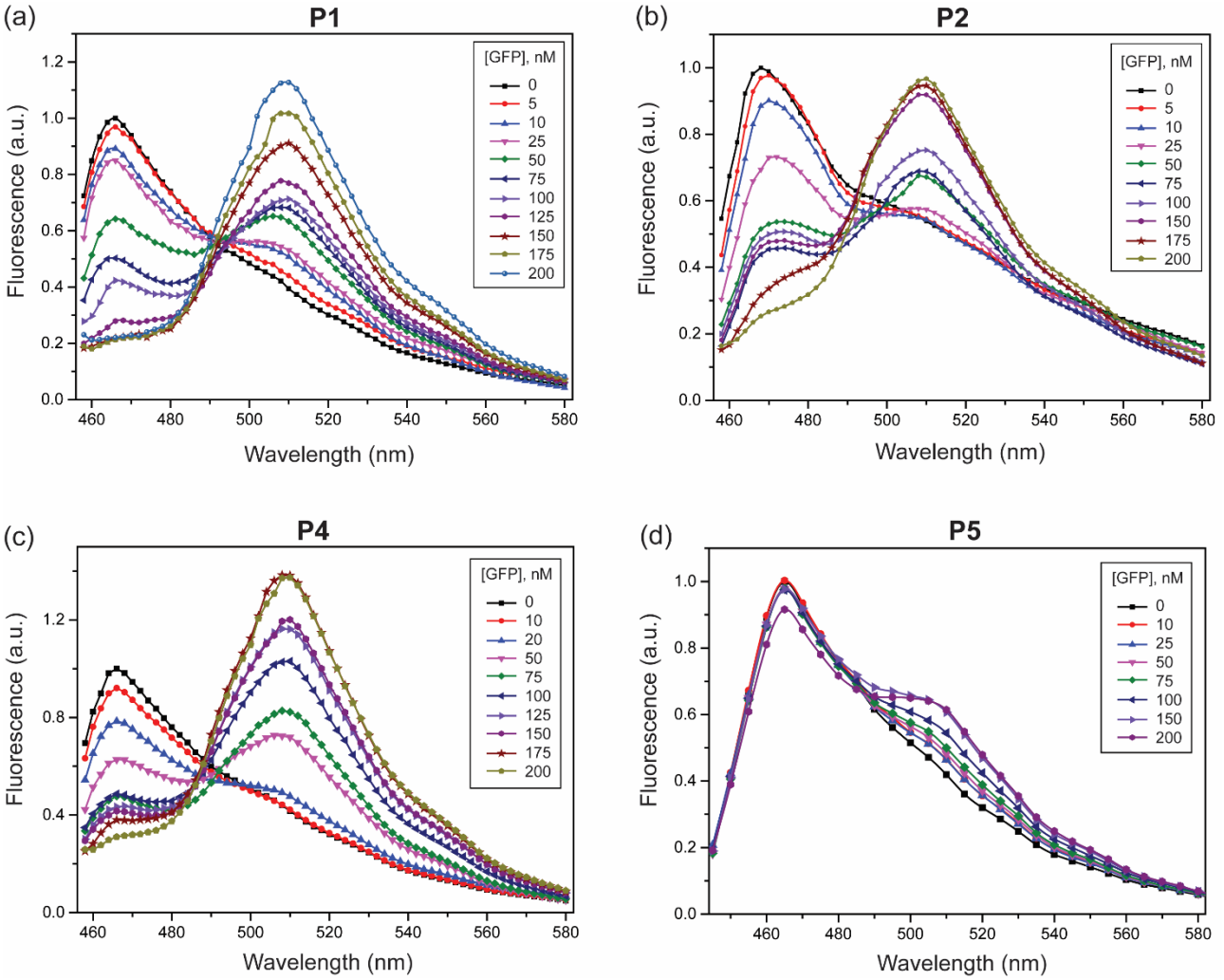

Figure S3. Emission spectra as a function of GFP concentration for the (a) **P1**-GFP, (b) **P2**-GFP, (c) **P4**-GFP and (d) **P5**-GFP pair. Spectra were recorded at an excitation of 430 nm following incubation of CPs and GFP in 5 mM sodium phosphate buffer (pH 7.4).

S7. Determination of FRET efficiency

We utilized the following equation[7] to calculate the experimental energy transfer efficiency (E):

$$E = \frac{(I_{\mathrm{CP}} - I_{\mathrm{CP-GFP}})}{I_{\mathrm{CP}}}$$

where I_{CP} and $I_{CP\text{-}GFP}$ are the fluorescence intensities of the CP donor alone and the CP in the presence of GFP acceptor, respectively.

Estimates of the CP–GFP separation distance R were calculated using the Förster formalism by fitting the above experimental FRET efficiencies E using the expression[8]:

$$R = \left(\frac{n\,(1-E)}{E}\right)^{1/6} R_0$$

where n is the number of GFP attached to the same polymer, R is the donor–acceptor separation, and R_0 is the Förster distance designating the donor–acceptor separation at 50% energy transfer efficiency. The Förster distance R_0 is determined from the equation[9]:

$$R_0 = 9.78 \times 10^3 [\kappa^2 \eta^{-4} Q_{\mathrm{CP}} J(\lambda)]^{1/6}$$

where η is the refractive index of the medium, Q_{CP} is the polymer quantum yield in the absence of acceptor, $J(\lambda)$ is the spectral overlap integral, and κ^2 is the dipole orientation factor. We used $\kappa^2 = 2/3$ corresponding to a random dipole orientation,[10] based on the assumption that in a polymer-protein pair it is impossible to control the relative orientation of the dipoles.

Figure S4 shows the data fitted as a function of n using the above expressions, and Table S3 lists the parameters determined for the various CP-GFP pairs.

Table S3. The data summary of spectral overlap integral (J), maximum energy transfer efficiency (E_{max}), Förster distance (R_0) and donor-acceptor distance (R).

Polymer	J (M^{-1} cm^{-1} nm^4)	R_0 (Å)	E_{max} (%)	R (Å)
P1	1.81×10^{15}	37.45	78	29.51
P2	1.57×10^{15}	43.40	70	38.24
P3	1.84×10^{15}	35.38	72	51.40
P4	1.92×10^{15}	47.37	60	53.41

The orientation factor $\kappa^2 = 2/3$ was used to calculate the R_0. Here, R values were obtained from fitting the data of FRET efficiency against CP to GFP ratio.

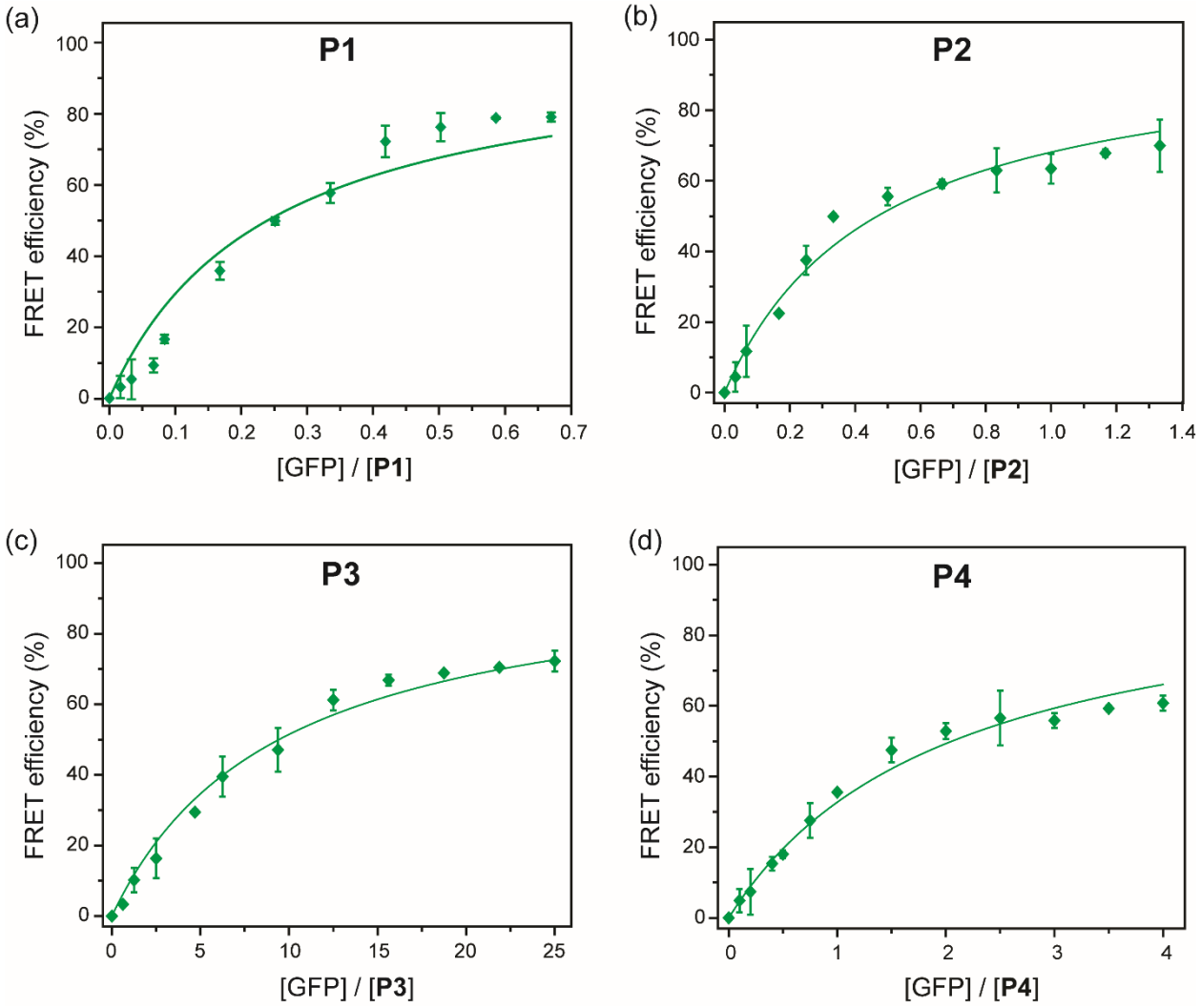

Figure S4. FRET efficiency (green squares) as a function of the increasing GFP concentration for (a) **P1**, (b) **P2**, (c) **P3**, and (d) **P4**. Each value is the average of three independent measurements and the error bars are the ± standard deviations (SD). Solid lines represent the best fitted curves obtained through fitting the Förster equation.

S8. Determination of binding affinities

Titration of CP by GFP results in FRET and the resulting fluorescence decay of CP as a function of GFP concentration was fitted to one-site binding equation,[11] which is:

$$I = I_0 + \frac{\alpha}{2}\left([\mathrm{P}]_0 + n[\mathrm{A}] + \frac{1}{K_s}\right) - \sqrt{\left\{\left([\mathrm{P}]_0 + n[\mathrm{A}] + \frac{1}{K_s}\right)^2 - 4n[\mathrm{P}]_0[\mathrm{A}]\right\}}$$

where, I_0 is the fluorescence intensity of a CP at a concentration $[\mathrm{P}]_0$ in the absence of acceptor (GFP), I is the fluorescence intensity of the CP in the presence of a concentration [A] of GFP, and n denotes the CP to GFP binding ratio, i.e. how many sites the GFP has to quench multiple PPE chains. The term α is the correlation factor between the fluorescence intensities and concentrations of the donor and acceptor species. This factor is constant if the instrumental variables (e.g. slit width, excitation wavelength, sensitivity, etc.) and the polymer and GFP identities are fixed.

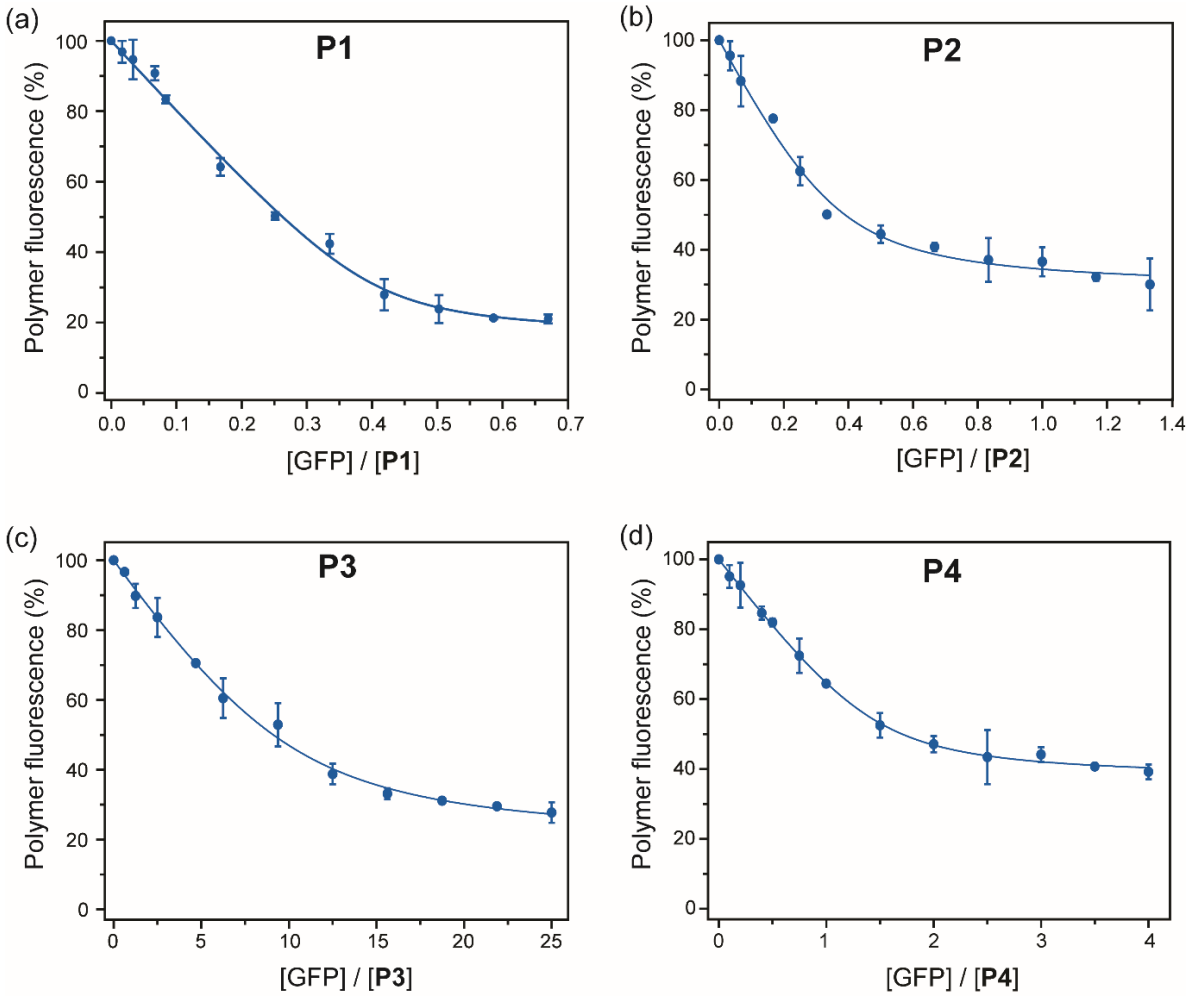

Figure S5. Quenching of CP fluorescence (blue circles) as a function of the increasing GFP concentration for (a) **P1**, (b) **P2**, (c) **P3**, and (d) **P4**. Each value is the average of three independent

measurements and the error bars are the ± SD. Solid lines represent the best fitted curves, obtained from fitting the binding equation using the model of single set of identical binding sites.

Table S4: CP-GFP complex stability constant (K_s) and CP to GFP binding stoichiometry (n) determined from fitting the fluorescence titration data

Polymers	K_s (M^{-1})	Binding ratio (n)
P1	9.13×10^7	2.5
P2	4.11×10^7	2.8
P3	6.78×10^8	0.1
P4	2.10×10^8	0.7

S9. Cell culture

All the cells were cultured at 37 °C under a humidified atmosphere containing 5% CO_2. Cells were regularly passaged by trypsinization with 0.25% trypsin-EDTA 1× solution (Invitrogen) in PBS (pH 7.4). HeLa, HepG2, MCF7, and NT2/D1 cells were cultured in DMEM media supplemented with 10% fetal bovine serum (FBS) and 1% antibiotics (Cellgro, 30-004-CI) in T75 flasks. CDβGeo, pTD, V14, and MCF10A cells were grown in DMEM-F12 media supplemented with 2% adult bovine serum (ABS), 25 mM HEPES, 10 mg/mL insulin, 5 ng/mL epidermal growth factor (EGF) and 15 mg/mL gentamicin. The NCI-H1299 (parental), and the Sublines were grown in RPMI-1640 media supplemented with 10% FBS and 1% antibiotic solution. CHO-K1, pgsB-618, pgsA-745, and pgsD-677 cells were cultured in Ham's nutrient mixture F12 supplemented with 10% FBS and 1% antibiotic solution (Cellgro, 30-004-CI).

Cells grown at ~80% confluence in the T75 flasks were washed twice with DPBS buffer (Thermo Scientific, SH30028.02), trypsinized, and collected in the respective growth medium. Thereafter, cells were spun down, resuspended in the medium (without serum/antibiotics), and counted using a hemocytometer. With appropriate dilutions the suspensions were used in the following cell sensing assays.

S10. Cell concentration-dependent FRET responses

The quantitative behavior of the sensor in cell sensing was determined in the same manner as the sensing studies. Cells were counted by a hemocytometer in triplicates and then serially diluted in the corresponding media. Fluorescence change was measured after 30 mins of incubation with the cells.

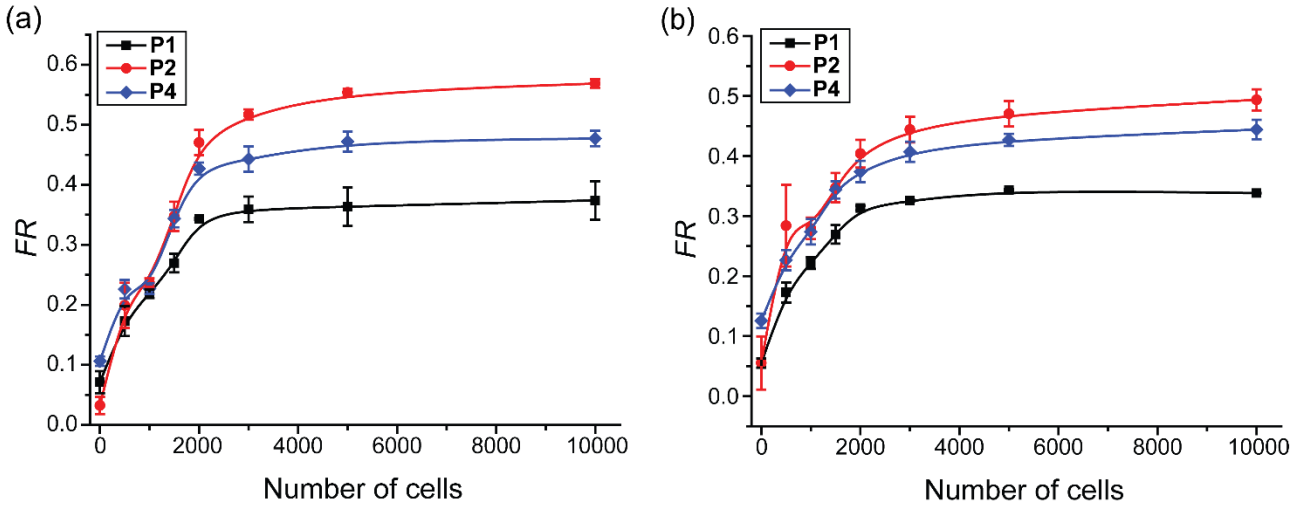

Figure S6. Change in the FRET response of the polymer **P1**, **P2**, and **P4** upon incubation with different number of (a) CHO-K1 and (b) pgsA-745 cells. Each value is the average of three independent measurements and the error bars are the ± SD. Solid lines are drawn to guide the eye.

A linear slope of FRET responses can be observed between 0 to 2000 cells, with a saturation at higher number of cells (Figure S6). The dose response behavior could be utilized for quantitatively detect cells within the observed dynamic range.

S11. Aggregation behavior of polymer on cell surfaces

Quenching of the polymers upon interaction with cell surfaces can be observed (see main text and reference 23 therein) that should arise from aggregation on cell surfaces. Confocal microscopy was employed to investigate the aggregation behavior of the polymers.

2.4×10^5 cells (CHO-K1, MCF-7, and pTD) were seeded into round bottom culture discs in the respective culture media and grown for 24 h at 37 °C. Cells were washed and the media was replaced with 1xPBS buffer. At this point, polymer solution was added (0.7 μM final concentration) to the cells and imaged after 15 min using Zeiss Meta 510 confocal laser scanning microscope.

The punctate patterns on the cell surfaces indicates aggregation of the polymer (Figure S7). The aggregation patterns appear to be dependent on cell type.

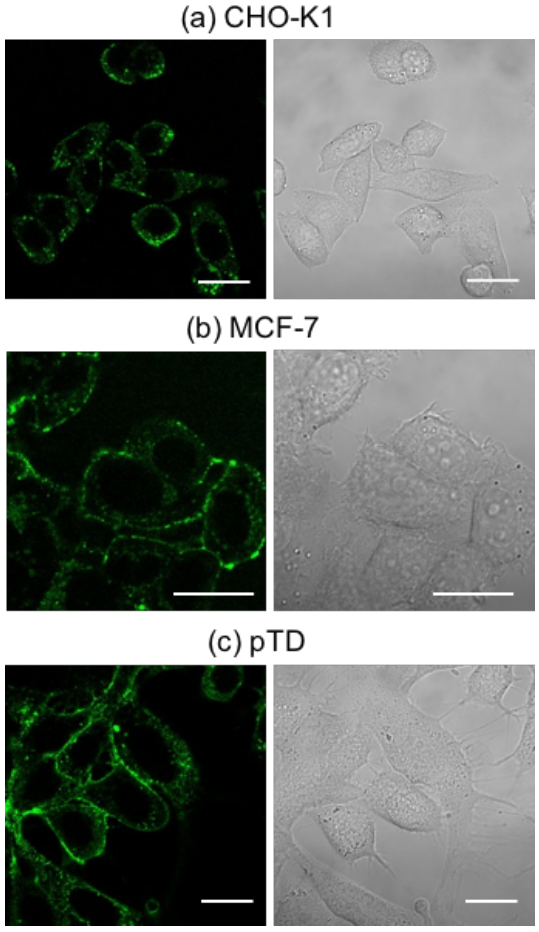

Figure S7. Confocal laser scanning micrograph (CLSM) showing the binding of **P1** to cell surfaces. Representative images collected in the polymer fluorescence channel and bright field are respectively presented for (a) CHO-K1, (b) MCF-7, and (c) pTD cells. Scale bars: 20 microns.

S12. Cell sensing

In the sensing studies, GFP and CPs (**P1-P4**) were mixed at stoichiometric ratio in 5 mM sodium phosphate buffer (pH 7.4). Each of the CP-GFP complexes (same concentration ratio as that of polymer–GFP titration, section S6) in multiple replicates were loaded (200 µL) into a black 96-well untreated plate (Costar) followed by incubation for 30 min at room temperature in dark. Fluorescence intensity was recorded on a Molecular Devices SpectraMax M5 microplate reader with excitation at 430 nm and cutoff at 455 nm, providing the fluorescence "without cells". Then, cell suspensions (20 µL, ~2000 cells) were added to each well of the plate containing the CP-GFP complexes, after which the fluorescence intensities were recorded at the same spectroscopic variables. The measured intensities provide the final fluorescence with cells.

S13. Statistical analysis

Linear discriminant analysis (LDA) models the similarities between the data corresponding to the same cluster by introducing the group classification into the data set. The data are then used as a training set to generate a linear discriminant (LD) function (also called canonical functions or factors) that describes the best fit parameters to separate different clusters (analytes). The discriminants are linear combinations of the measured (independent) variables such as the sensor responses. Discriminant functions are calculated with the objective of maximizing the distance between classes relative to the variation within classes. The first discriminant is the linear combination of the variables that best discriminates among the groups; the second discriminant is orthogonal to the first and is the next best combination of variables, and so on. First discriminant function:

$$LD = c + a_1x_1 + a_2x_2 + ... + a_nx_n$$

where, a_1 through a_n are discriminant coefficients, x_1 through x_n are discriminating variables, and c is a constant. In the discriminant score plot each response pattern generated can be reduced to a single score and plotted in the new discriminant space.

The jackknifed classification matrix presents the outcome of cross-validation (leave-one-out) routine in LDA. The analysis validates the correctness of sample classification by the sensor array by leaving out one sample observation of the set at a time, and uses the rest of the data as a training set to generate the discriminant function. The discriminant function is then used to reclassify the excluded observation within the correct cluster. This is performed for each observation, and the overall ability to classify the observations describes the quality and predictability of the array.

In the present analyses, classical LDA were performed using Systat (version 11.0) program.[12] Herein, all variables were used in the model (complete mode) and the tolerance was set to 0.001. The raw fluorescence responses were transformed to canonical scores setting the cell types as the grouping variable. These canonical scores were further plotted as scatterplot with 95% confidence ellipse. In the LD multidimensional space, the Mahalanobis distance is a measure of the distance of a data point to the centroid of a training group[13] that can be calculated using *discrim* function in Systat. The identity of an unknown was predicted by deducing the Mahalanobis distance of the unknown data from the training groups. The unknowns were assigned to the cell type from which the distance was the shortest.

Hierarchical clustering analysis (HCA) on the data set was performed using the *hclust* function of the stats package of R assuming a complete linkage method.[14] *hclust* begins with each case serving as its own cluster and the two most similar cases or clusters are joined at each step in the clustering process. This process iterates until all cases fall into a single cluster.

(a)

	A	B	C	% correct
A	8	0	0	100
B	0	8	0	100
C	0	0	8	100
Total	8	8	8	100

A : CDβGeo B : pTD C : V14

(b)

	D	E	F	G	% correct
D	8	0	0	0	100
E	0	8	0	0	100
F	0	0	8	0	100
G	0	0	0	8	100
Total	8	8	8	8	100

D : NCI-H1299 F : Subline-2
E : Subline-1 G : Subline-5

(c)

	H	I	J	K	L	% correct
H	6	0	0	0	0	100
I	0	6	0	0	0	100
J	0	0	6	0	0	100
K	0	0	0	6	0	100
L	0	0	0	0	6	100
Total	6	6	6	6	6	100

H : HepG2 J : NT2 L : HeLa
I : MCF7 K : MCF10A

(d)

	M	N	O	P	% correct
M	8	0	0	0	100
N	0	8	0	0	100
O	0	0	8	0	100
P	0	0	0	8	100
Total	8	8	8	8	100

M : CHO-K1 O : pgsB-618
N : pgsA-745 P : pgsD-677

Figure S8: leave-one-out cross-validation analysis by Jackknifing in LDA for (a) murine mammary, (b) human NSCLC parental and site-specific metastatic, (c) human, and (d) CHO cell types.

S14. Fingerprinting of human cell types

Table S5: Features of the human cell lines used in the study

Cell line	Tissue origin	Features of the cell lines	Cell status
MCF10A	Breast	Epithelial cells	Non-tumorigenic
HeLa	Cervix	Epithelial cells	Tumorigenic
HepG2	Liver	Epithelial cells	Tumorigenic
NT2/D1	Testis	Epithelial-like cells; derived from metastatic site (lung)	Tumorigenic
MCF7	Breast	Epithelial cell; derived from metastatic site (pleural effusion)	Tumorigenic

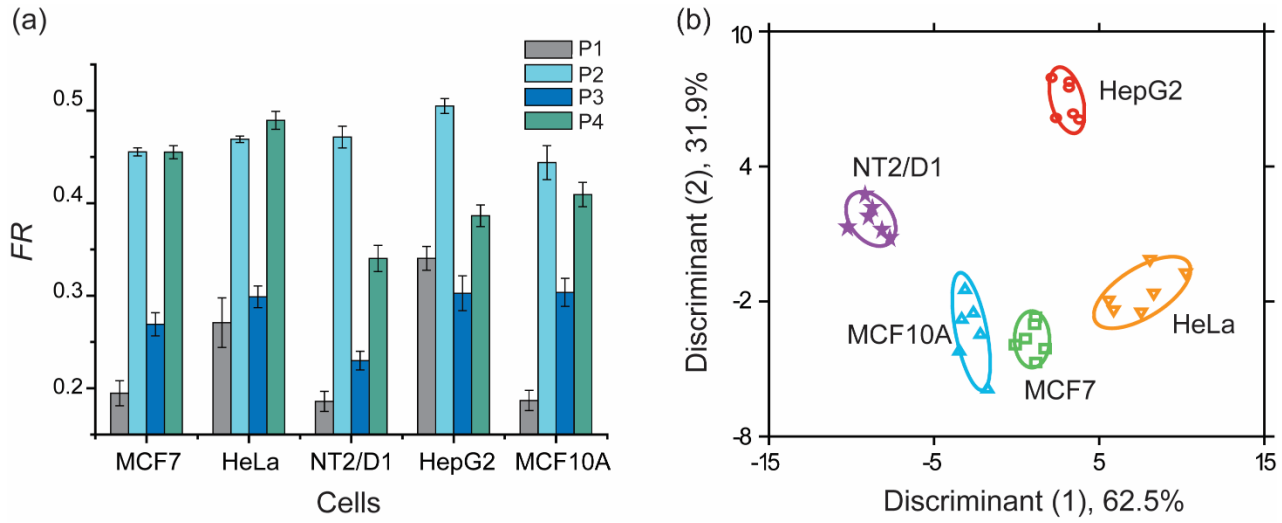

Figure S9. Detection of human cell types. (a) Change in FRET responses (*FR*) from the polymer-GFP complexes upon interaction with the five human cell types, where each value is the average of six independent measurements and the error bars are the ± SD. (b) LDA score plot of the fluorescence responses. The analysis resulted in canonical scores with three discriminants explaining 62.5%, 31.9%, and 5.6% of total variance and was plotted with 95% confidence ellipses around the centroid of each group.

S15. Glycomutant CHO cells: FRET responses

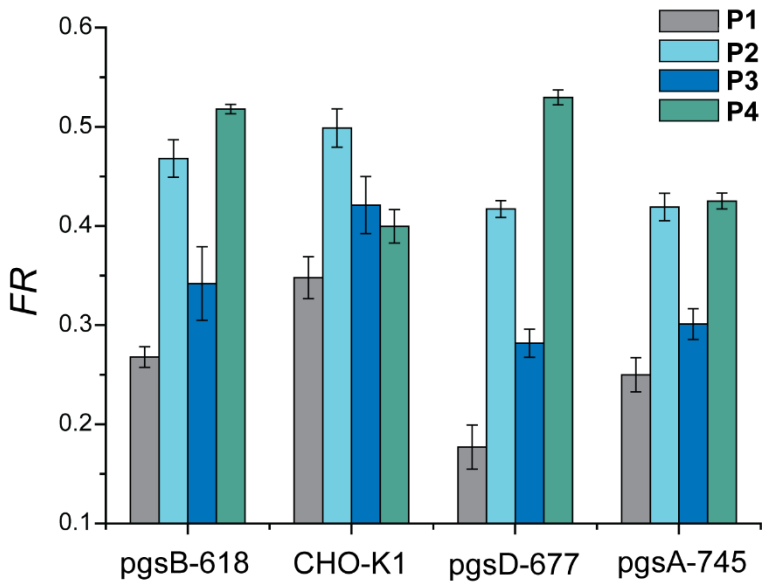

Figure S10: Change in FRET responses (*FR*) from the sensor upon interacting with the CHO cell types, where each value is the average of eight independent measurements and the error bars are the ± SD.

S16. Contribution of CPs towards the differential FRET responses

Evaluating the contribution of each CP in the sensor output would validate their importance in generating the sensor array. Pearson's correlation was performed using Systat software.

It can be observed that depending on the cell types different CPs contribute to the discriminants to a different extent. However, all the polymers had significant correlation with the discriminants.

(a) Murine isogenic mammary cell types

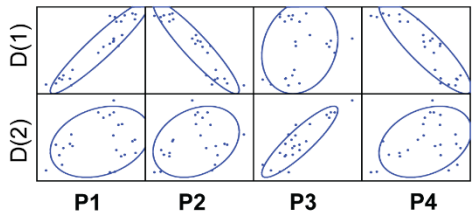

	P1	P2	P3	P4
D(1)	0.941	-0.927	0.182	-0.882
D(2)	0.268	0.279	0.890	0.316

(b) Human NSCLC site-specific metastatic cell types

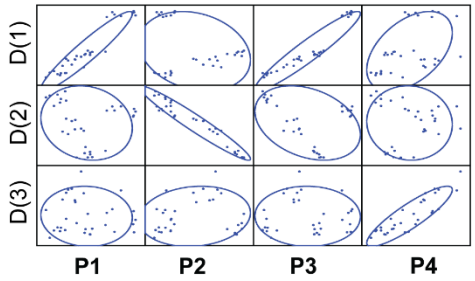

	P1	P2	P3	P4
D(1)	0.944	-0.220	0.946	0.466
D(2)	-0.138	-0.965	-0.312	-0.040
D(3)	-0.046	0.117	-0.017	0.881

(c) Human cell types

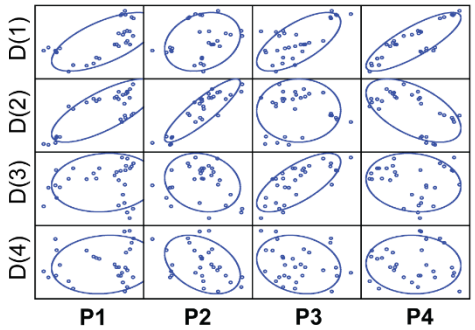

	P1	P2	P3	P4
D(1)	0.652	0.234	0.679	0.820
D(2)	0.743	0.883	0.008	-0.558
D(3)	0.099	-0.170	0.707	-0.197
D(4)	0.116	-0.370	-0.197	-0.042

(d) Glycomutant CHO cell types

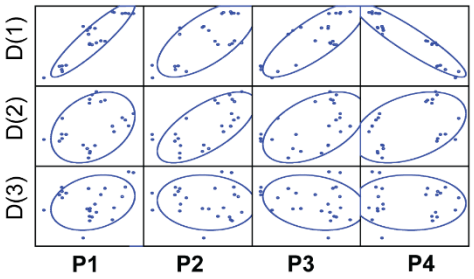

	P1	P2	P3	P4
D(1)	0.825	0.565	0.668	-0.915
D(2)	0.408	0.733	0.583	0.400
D(3)	0.390	-0.251	-0.365	0.015

Figure S11. Pearson's correlation coefficients between the FRET responses and the discriminant scores generated by LDA. Here, D refers to the discriminants. The coefficients highlighted in green are the contributions of the corresponding polymers towards one discriminant.

Next, we investigated whether or not different all CP-GFP complexes provide equivalent or better classification efficiency than the combination of the four CPs using LDA on the fluorescence responses from different FP pairs (Figure S10a). In addition, identification of unknowns using the best differentiating CP-GFP combinations (Figure S10b) to verify the importance of each of the

polymers in sensor array.

(a) Jackknifed classification matrix

Polymers				% Correct classification			
P1	**P2**	**P3**	**P4**	Murine mammary	Site-specific metastatic	Human	Glycomutant CHO
■				79	84	57	83
	■			92	72	77	46
		■		58	100	60	67
			■	75	50	93	75
■			■	100	100	100	100
	■		■	92	100	97	100
		■	■	88	100	87	96
■	■			100	100	87	100
■		■		88	100	90	92
	■	■		96	100	90	79
■	■		■	100	100	100	100
■		■	■	100	100	100	100
■	■	■	■	100	100	100	100

(b) Identification of unknown samples

Polymers				% Correct identification of cell types*			
P1	**P2**	**P3**	**P4**	Murine mammary	Site-specific metastatic	Human	Glycomutant CHO
■			■	79.1 (19/24)	65.6 (21/32)	76.6 (23/30)	53.1 (17/32)
■	■		■	91.6 (22/24)	84.3 (27/32)	86.6 (26/30)	84.3 (27/32)
■		■	■	83.3 (20/24)	78.1 (25/32)	73.3 (22/30)	65.6 (21/32)
■	■	■	■	95.8 (23/24)	100 (32/32)	90.0 (27/30)	90.6 (29/32)

* in the parentheses: correctly identified/total number of samples

Figure S12. (a) Jackknifed classification matrix obtained through LDA on the FRET responses for all the cell types. Different CP-GFP combinations were used to pick out the combinations with the best differentiation. (b) Identification of the unknowns using the CP-GFP combinations that provided the maximum separation across the cell types.

It is readily observed that the four CPs together provide the maximum efficiency of unknown identification. Overall, importance of each CP in the current biosensor array can be envisaged in classifying different types of cells and identifying the blinded unknowns.

S17. Glyco-mutant cell sensing using polymer only

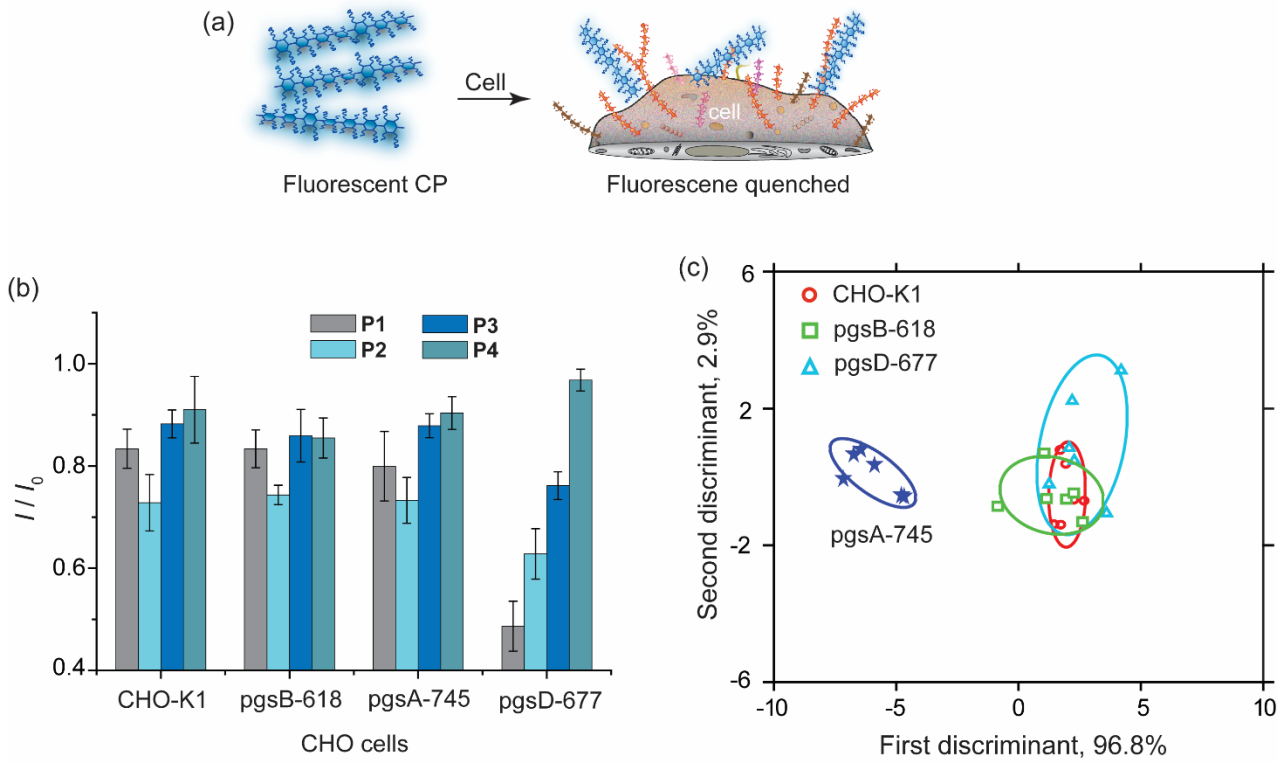

Figure S13. Detection of glyco-engineered cells using CPs only. (a) Schematic representation of the interaction of the polymers alone with cells, resulting in fluorescence quenching. (b) Change in fluorescence intensity of the polymers upon interaction with the parental and GAG-mutated cells, where I and I_0 are respectively the fluorescence with and without the cells. The data are average of six independent replicates and the error bars represent the ±SD. The experiment was performed simultaneously with the FRET system using the same set of cells. (c) LDA score plot of the fluorescence changes. The analysis resulted in canonical scores with three discriminants explaining 96.8%, 2.9%, and 0.3% of total variance and was plotted with 95% confidence ellipses around the centroid of each group.

S18. FRET response data for the training and test sets

Table S6. FRET responses and the LDA output obtained from the murine isogenic healthy, cancerous, and metastatic mammary cell types.

Cells	*FR*				LDA output	
	P1	P2	P3	P4	Score(1)	Score(2)
CDβGeo	0.2280	0.4871	0.3222	0.4729	-6.8439	1.0188
CDβGeo	0.2295	0.4808	0.3043	0.4539	-5.8071	-0.1338
CDβGeo	0.2350	0.4823	0.2817	0.4899	-7.0516	0.0101
CDβGeo	0.2608	0.4874	0.3146	0.4724	-5.3393	1.3152
CDβGeo	0.2525	0.4969	0.3023	0.4836	-6.6424	1.1708
CDβGeo	0.2749	0.5025	0.3221	0.4962	-6.2921	2.6488
CDβGeo	0.2715	0.5015	0.2918	0.4641	-5.2851	0.7725
CDβGeo	0.2862	0.5132	0.3086	0.5022	-6.5517	2.7008
pTD	0.3010	0.4306	0.2462	0.4467	0.0264	-2.0372
pTD	0.3127	0.4219	0.2379	0.4374	1.3137	-2.4998
pTD	0.2776	0.4482	0.2109	0.4388	-1.7172	-3.5408
pTD	0.2669	0.4170	0.2976	0.4311	-0.1469	-1.4235
pTD	0.2865	0.4430	0.2502	0.4307	-0.6289	-2.2820
pTD	0.2784	0.4340	0.2982	0.4479	-1.0650	-0.5018
pTD	0.2585	0.4418	0.2760	0.4484	-2.4562	-1.4787
pTD	0.2775	0.4387	0.2438	0.4412	-1.2550	-2.5017
V14	0.3949	0.4092	0.3486	0.4131	7.0014	2.0527
V14	0.4313	0.4145	0.3359	0.4221	8.0535	2.5370
V14	0.4088	0.3883	0.2921	0.4306	7.8219	0.3049
V14	0.3740	0.3597	0.3090	0.4151	8.2299	-0.5864
V14	0.3770	0.3927	0.3137	0.4142	6.8180	0.2261
V14	0.3712	0.4077	0.3000	0.4362	4.9511	0.4162
V14	0.4013	0.4048	0.3131	0.4303	6.7512	1.2159
V14	0.3919	0.4242	0.3030	0.4099	6.1154	0.5959

Table S7. FRET responses and the LDA output obtained from the isogenic human NSCLC site-specific metastatic cells.

Cells	*FR*				LDA output		
	P1	P2	P3	P4	Score(1)	Score(2)	Score(3)
NCI-H1299	0.3545	0.5652	0.2824	0.4207	-13.1734	-2.5509	-0.2951
NCI-H1299	0.3349	0.5899	0.2667	0.4095	-15.0856	-3.4408	-0.6537
NCI-H1299	0.2580	0.5187	0.2705	0.4193	-15.4893	-1.4924	-0.4532
NCI-H1299	0.2569	0.5709	0.2874	0.4663	-15.0392	-2.9226	1.6351
NCI-H1299	0.2599	0.5211	0.2753	0.4485	-14.8575	-1.2480	0.8364
NCI-H1299	0.3271	0.5804	0.2724	0.4606	-14.1513	-2.5723	1.5914
NCI-H1299	0.2514	0.5347	0.3072	0.4444	-13.8187	-2.3358	0.4072
NCI-H1299	0.3038	0.5521	0.3086	0.3781	-13.5554	-3.4665	-2.5171
Subline-1	0.5451	0.5347	0.5726	0.5075	8.0322	-3.5765	1.4629
Subline-1	0.5737	0.5565	0.6250	0.4704	10.4856	-5.4464	-0.5686
Subline-1	0.5012	0.5326	0.6152	0.4906	8.7718	-4.7323	0.3010
Subline-1	0.5232	0.5355	0.6142	0.5168	9.6131	-4.3021	1.5283
Subline-1	0.5322	0.5812	0.6210	0.5078	9.2093	-6.0270	1.1550
Subline-1	0.5601	0.5990	0.5962	0.5246	8.6196	-5.8109	2.1852
Subline-1	0.5201	0.5556	0.6108	0.5077	8.8597	-5.0797	1.1732
Subline-1	0.5045	0.5943	0.6307	0.5153	8.8009	-6.7317	1.4127
Subline-2	0.4938	0.3521	0.4740	0.4092	3.8978	2.5414	-2.5862
Subline-2	0.5008	0.4462	0.4901	0.4149	3.1912	-0.8046	-2.2795
Subline-2	0.5142	0.3689	0.5045	0.4350	5.9788	1.9774	-1.6093
Subline-2	0.4375	0.3369	0.5453	0.4317	6.5047	1.8176	-2.2345
Subline-2	0.4472	0.3592	0.4813	0.3717	2.3747	1.3383	-4.3867
Subline-2	0.4694	0.3828	0.4830	0.4335	3.4364	1.4966	-1.5305
Subline-2	0.4809	0.4075	0.5327	0.4159	5.5018	-0.2932	-2.6721
Subline-2	0.4683	0.4349	0.5037	0.4391	3.5283	-0.5476	-1.3488
Subline-5	0.4232	0.2487	0.3828	0.4517	0.0042	7.5890	-0.1920
Subline-5	0.4346	0.2834	0.4100	0.4963	1.5983	6.6577	1.6908
Subline-5	0.4144	0.2762	0.4011	0.4996	0.7982	6.9392	1.8738
Subline-5	0.4150	0.2839	0.4208	0.5017	1.6699	6.3960	1.8274

Subline-5	0.4072	0.2554	0.3946	0.4862	0.4932	7.5216	1.2745
Subline-5	0.4312	0.3137	0.4197	0.4889	1.3171	5.3385	1.3256
Subline-5	0.4635	0.2568	0.4003	0.4737	2.0929	7.6252	0.7268
Subline-5	0.3594	0.2707	0.4248	0.4844	0.3911	6.1429	0.9202

Table S8. FRET responses and the LDA output obtained from human normal, cancerous, and metastatic cells.

Cell	*FR*				LDA output			
	P1	P2	P3	P4	Score(1)	Score(2)	Score(3)	Score(4)
HeLa	0.3081	0.4668	0.3089	0.5004	10.245	-0.783	-0.354	0.956
HeLa	0.2985	0.4663	0.2840	0.4822	8.073	-0.186	-1.545	1.372
HeLa	0.2554	0.4695	0.3005	0.4975	7.546	-2.522	-0.977	-0.407
HeLa	0.2434	0.4683	0.2867	0.4855	5.877	-2.429	-1.545	-0.282
HeLa	0.2497	0.4682	0.2994	0.4761	5.572	-1.994	-0.385	-0.323
HeLa	0.2702	0.4760	0.3134	0.4958	8.304	-1.684	-0.314	-0.738
HepG2	0.3509	0.5021	0.2921	0.3710	2.154	7.915	0.659	0.748
HepG2	0.3267	0.4999	0.2971	0.3880	2.422	6.130	0.616	0.060
HepG2	0.3611	0.5010	0.3232	0.3742	3.221	7.744	2.786	0.409
HepG2	0.3336	0.5059	0.3220	0.3973	3.823	6.057	1.823	-0.759
HepG2	0.3346	0.5005	0.2742	0.3998	3.452	6.325	-1.347	0.646
HepG2	0.3360	0.5210	0.3072	0.3883	3.208	7.488	0.397	-1.374
MCF7	0.2108	0.4580	0.2762	0.4473	1.149	-2.698	-0.740	0.027
MCF7	0.2019	0.4491	0.2836	0.4598	1.728	-4.094	-0.199	0.179
MCF7	0.1782	0.4574	0.2723	0.4668	1.158	-4.714	-1.546	-0.812
MCF7	0.1865	0.4610	0.2654	0.4547	0.534	-3.647	-1.838	-0.626
MCF7	0.1838	0.4517	0.2468	0.4524	-0.084	-3.922	-2.660	0.350
MCF7	0.2067	0.4557	0.2704	0.4501	1.093	-3.011	-1.127	0.186
NT2	0.1978	0.4679	0.2288	0.3352	-8.735	2.159	-1.254	0.660
NT2	0.1888	0.4510	0.2356	0.3224	-10.249	1.296	0.315	1.525
NT2	0.1951	0.4751	0.2105	0.3331	-9.173	2.756	-2.780	0.494
NT2	0.1879	0.4701	0.2301	0.3375	-8.972	1.782	-1.328	0.209

NT2	0.1708	0.4832	0.2366	0.3611	-7.682	0.829	-2.113	-1.410
NT2	0.1746	0.4816	0.2373	0.3529	-8.156	1.195	-1.767	-1.170
MCF10A	0.2023	0.4428	0.2979	0.4031	-2.619	-2.457	2.696	0.650
MCF10A	0.1934	0.4376	0.2824	0.4166	-2.194	-3.406	1.456	1.028
MCF10A	0.1842	0.4262	0.2995	0.4046	-3.476	-4.145	3.484	1.283
MCF10A	0.1789	0.4606	0.3286	0.4008	-3.326	-2.739	4.128	-1.827
MCF10A	0.1716	0.4254	0.3046	0.4330	-1.762	-5.831	3.060	0.739
MCF10A	0.1902	0.4706	0.3090	0.3984	-3.128	-1.414	2.399	-1.791

Table S9. FRET responses and the LDA output obtained from the glyco-mutant Chinese hamster ovary cells.

Cells	***FR***				**LDA output**		
	P1	**P2**	**P3**	**P4**	**Score(1)**	**Score(2)**	**Score(3)**
CHO-K1	0.2839	0.4893	0.4860	0.4462	5.9525	1.7935	-2.4950
CHO-K1	0.3475	0.4919	0.4424	0.4311	7.8344	1.9170	-0.2380
CHO-K1	0.3411	0.4913	0.3814	0.4143	7.8769	0.3988	0.1969
CHO-K1	0.3404	0.4688	0.4432	0.4366	6.9720	1.4109	0.0901
CHO-K1	0.3397	0.4582	0.4079	0.4201	7.4623	0.0285	0.5594
CHO-K1	0.2954	0.4951	0.3707	0.4311	5.3767	0.2470	-0.8958
CHO-K1	0.2854	0.5228	0.4716	0.4259	7.7137	1.6985	-3.2126
CHO-K1	0.3893	0.5224	0.4196	0.4467	7.5623	3.9074	0.8909
pgsA-745	0.2504	0.4320	0.3312	0.4359	2.4674	-2.5007	-0.3331
pgsA-745	0.2620	0.4009	0.3010	0.4179	3.1946	-4.2095	0.8453
pgsA-745	0.2479	0.4176	0.2880	0.4154	3.0355	-4.2738	0.2178
pgsA-745	0.2594	0.4141	0.2992	0.4109	3.8075	-4.2208	0.4267
pgsA-745	0.2658	0.4374	0.2949	0.4446	1.5626	-2.1072	0.6216
pgsA-745	0.2777	0.3989	0.2922	0.4328	2.2216	-3.4418	1.6688
pgsA-745	0.2595	0.4102	0.3327	0.4545	0.9953	-2.1126	0.6125
pgsA-745	0.2664	0.4340	0.3384	0.4251	3.8268	-2.5280	-0.1298
pgsB-618	0.3015	0.4375	0.3048	0.5130	-2.7206	1.5496	2.4313
pgsB-618	0.2834	0.4522	0.3045	0.5099	-2.7214	1.4734	1.5451

pgsB-618	0.2649	0.4408	0.3770	0.5230	-2.9949	2.1832	0.4087
pgsB-618	0.2458	0.4527	0.3620	0.5159	-3.0098	1.6824	-0.3005
pgsB-618	0.2725	0.4545	0.3866	0.5094	-1.4241	2.2213	0.0470
pgsB-618	0.2691	0.4854	0.3371	0.5237	-3.1168	3.0377	0.1555
pgsB-618	0.2999	0.4458	0.3363	0.5235	-2.8974	2.5331	1.9159
pgsB-618	0.3117	0.4855	0.3606	0.5136	-0.9265	3.6607	0.9852
pgsD-677	0.2007	0.4351	0.3200	0.5396	-6.8610	0.9157	-0.4149
pgsD-677	0.1539	0.4258	0.2792	0.5339	-8.3536	-0.8882	-1.1455
pgsD-677	0.1608	0.4281	0.3213	0.5126	-5.7591	-1.1321	-1.8305
pgsD-677	0.1782	0.4058	0.2805	0.5221	-7.1056	-1.4563	-0.1662
pgsD-677	0.1479	0.4150	0.2800	0.5202	-7.5532	-1.8560	-1.2862
pgsD-677	0.1697	0.4118	0.2885	0.5527	-9.4485	-0.0737	-0.2648
pgsD-677	0.2047	0.4160	0.3035	0.5270	-6.3302	-0.2340	0.1673
pgsD-677	0.1837	0.4298	0.3337	0.5340	-6.6395	0.3760	-1.0730

Table S10. Identification of the blinded unknowns from the murine healthy, cancerous, and metastatic cells using the FRET sensor. LDA was performed on the fluorescence responses of the training set and the unknowns at the same time, and the Mahalanobis distance of each unknown from the centroid of training groups was calculated. The training set included all the five human cell types. Based on the shortest Mahalanobis distance (data that are green colored) from a training group, an unknown is assigned to that particular group. Wrong identifications are red colored. Distance from the groups: d(1) = CDβGeo; d(2) = V14; d(3) = pTD cells.

Unknown sample #	*FR*				(Mahalanobis distance)^2			Predicted as	Accuracy of identification
	P1	P2	P3	P4	d(1)	d(2)	d(3)		
1	0.3262	0.4354	0.2268	0.5441	88.65	170.51	83.50	pTD	Yes
2	0.3214	0.5053	0.3811	0.4944	24.01	142.96	68.35	CDβGeo	Yes
3	0.2766	0.4900	0.3684	0.5037	13.98	177.71	68.94	CDβGeo	Yes
4	0.4458	0.4218	0.3699	0.4172	231.95	15.33	127.32	V14	Yes
5	0.2342	0.3891	0.3434	0.4921	64.56	139.08	59.31	pTD	Yes
6	0.2714	0.5001	0.3171	0.5188	11.68	212.82	73.76	CDβGeo	Yes
7	0.2836	0.4920	0.3401	0.5043	8.95	168.92	57.26	CDβGeo	Yes

8	0.3637	0.3447	0.3148	0.4421	211.26	22.71	92.20	V14	Yes
9	0.3099	0.4414	0.3452	0.4768	35.93	70.73	26.50	pTD	Yes
10	0.3963	0.3887	0.3916	0.4175	213.17	12.89	111.01	V14	Yes
11	0.3248	0.4387	0.2724	0.4405	57.05	37.92	5.58	pTD	Yes
12	0.3333	0.3799	0.2903	0.4621	116.19	31.63	38.61	V14	No
13	0.3116	0.4001	0.2020	0.4950	96.64	102.73	42.14	pTD	Yes
14	0.3110	0.4083	0.2164	0.5316	103.39	156.73	77.65	pTD	Yes
15	0.3783	0.3201	0.3806	0.4474	289.31	53.01	164.19	V14	Yes
16	0.3333	0.5137	0.3079	0.5133	18.82	157.57	60.36	CDβGeo	Yes
17	0.3989	0.2136	0.3625	0.4146	630.37	199.52	405.87	V14	Yes
18	0.3642	0.2565	0.3552	0.4141	440.90	107.35	256.40	V14	Yes
19	0.3359	0.3290	0.3468	0.4142	232.68	27.55	105.02	V14	Yes
20	0.3008	0.4890	0.3811	0.4745	19.81	122.75	50.67	CDβGeo	Yes
21	0.3233	0.3930	0.2137	0.4606	106.77	53.96	25.95	pTD	Yes
22	0.2642	0.5019	0.3285	0.4716	2.24	166.14	44.16	CDβGeo	Yes
23	0.2488	0.4920	0.3948	0.5046	21.74	221.00	94.60	CDβGeo	Yes
24	0.3581	0.2324	0.3900	0.4278	505.03	159.62	321.68	V14	Yes

Table S11. Identification of the blinded unknowns from the human isogenic site-specific NSCLC metastatic cell lines using the FRET sensor. LDA was performed on the fluorescence responses of the training set and the unknowns at the same time, and the Mahalanobis distance of each unknown from the centroid of training groups was calculated. The training set included all the four murine cell types. Based on the shortest Mahalanobis distance (data that are green colored) from a training group, an unknown is assigned to that particular group. Wrong identifications are red colored. Distance from the groups: d(1) = NCI-H1299; d(2) = Subline-1; d(3) = Subline-2; d(4) = Subline-5.

Unknown sample #	***FR***				**(Mahalanobis distance)^2**				**Predicted as**	**Accuracy of identification**
	P1	**P2**	**P3**	**P4**	**d(1)**	**d(2)**	**d(3)**	**d(4)**		
1	0.5470	0.5294	0.5924	0.4604	0.5470	5.08	48.24	183.82	Subline-1	Yes
2	0.2380	0.5284	0.2688	0.4011	0.2380	670.89	446.72	397.09	NCI-H1299	Yes
3	0.5296	0.3641	0.5659	0.4806	0.5296	52.88	40.23	107.92	Subline-2	Yes
4	0.5231	0.5493	0.6102	0.4533	0.5231	6.44	59.49	211.21	Subline-1	Yes

5	0.5272	0.5305	0.6099	0.4947	0.5272	1.18	61.20	192.00	Subline-1	Yes
6	0.4926	0.3544	0.5630	0.4980	0.4926	56.33	37.76	91.45	Subline-2	Yes
7	0.2322	0.5281	0.3328	0.4017	0.2322	527.95	341.96	327.75	NCI-H1299	Yes
8	0.5291	0.5811	0.5951	0.4970	0.5291	2.24	67.08	202.15	Subline-1	Yes
9	0.2347	0.5311	0.3018	0.3612	0.2347	633.40	418.71	403.69	NCI-H1299	Yes
10	0.5282	0.5685	0.5844	0.5024	0.5282	2.72	59.05	182.53	Subline-1	Yes
11	0.2825	0.5404	0.2924	0.3922	0.2825	570.14	368.70	342.64	NCI-H1299	Yes
12	0.2586	0.5332	0.3316	0.3917	0.2586	507.85	324.34	316.84	NCI-H1299	Yes
13	0.4120	0.2932	0.4637	0.5539	0.4120	159.62	66.00	19.12	Subline-5	Yes
14	0.4651	0.3305	0.4665	0.5255	0.4651	120.87	39.91	19.84	Subline-5	Yes
15	0.2941	0.5418	0.2459	0.4296	0.2941	644.37	427.02	361.50	NCI-H1299	Yes
16	0.2395	0.5354	0.2636	0.4469	0.2395	654.59	441.69	373.32	NCI-H1299	Yes
17	0.5324	0.4066	0.5408	0.4973	0.5324	40.77	28.60	87.04	Subline-2	Yes
18	0.3553	0.2410	0.4389	0.5326	0.3553	218.78	81.19	10.25	Subline-5	Yes
19	0.5394	0.5582	0.6217	0.4506	0.5394	7.13	71.58	234.51	Subline-1	Yes
20	0.4955	0.3591	0.5165	0.5160	0.4955	72.41	31.97	53.88	Subline-2	Yes
21	0.5161	0.3480	0.5264	0.5217	0.5161	77.85	45.75	69.80	Subline-2	Yes
22	0.2654	0.5558	0.2883	0.4204	0.2654	590.91	395.62	358.98	NCI-H1299	Yes
23	0.5370	0.3896	0.5647	0.4835	0.5370	41.88	37.02	110.23	Subline-2	Yes
24	0.5137	0.3569	0.5523	0.4970	0.5137	59.07	37.96	88.37	Subline-2	Yes
25	0.4705	0.2761	0.4476	0.5233	0.4705	167.35	61.34	17.51	Subline-5	Yes
26	0.4453	0.2270	0.4115	0.5411	0.4453	245.16	105.03	18.88	Subline-5	Yes
27	0.5172	0.4005	0.5467	0.4968	0.5172	40.17	27.28	86.42	Subline-2	Yes
28	0.4401	0.2378	0.4524	0.5440	0.4401	199.98	87.49	25.75	Subline-5	Yes
29	0.4414	0.2583	0.4390	0.5424	0.4414	195.78	80.12	16.94	Subline-5	Yes
30	0.5394	0.5991	0.5839	0.4893	0.5394	6.12	68.39	205.71	Subline-1	Yes
31	0.5196	0.5715	0.5969	0.4823	0.5196	3.45	61.32	199.80	Subline-1	Yes
32	0.4325	0.2584	0.4580	0.5529	0.4325	184.62	81.88	24.65	Subline-5	Yes

Table S12. Identification of the blinded unknowns from the glyco-mutated cells using the FRET sensor. LDA was performed on the fluorescence responses of the training set and the unknowns at the same time, and the Mahalanobis distance of each unknown from the centroid of training groups was calculated. The training set included all the five human cell types. Based on the shortest Mahalanobis distance (data that are green colored) from a training group, an unknown is assigned to that particular group. Wrong identifications are red colored. Distance from the groups: d(1) = CHO-K1; d(2) = pgsA-745; d(3) = pgsB-618; d(4) = pgsD-677 cells.

Unknown sample #	*FR*				(Mahalanobis distance)^2				Predicted as	Accuracy of identification
	P1	P2	P3	P4	d(1)	d(2)	d(3)	d(4)		
1	0.3917	0.3690	0.3110	0.4585	76.78	45.67	74.06	156.75	pgsA-745	Yes
2	0.3626	0.4756	0.4298	0.4540	7.02	46.30	73.17	189.61	CHO-K1	Yes
3	0.2855	0.4301	0.3195	0.5733	232.82	158.38	32.59	31.63	pgsD-677	No
4	0.2686	0.4441	0.3200	0.5462	169.56	104.68	10.88	18.06	pgsB-618	Yes
5	0.3668	0.4942	0.4176	0.4420	3.19	51.68	90.18	215.35	CHO-K1	Yes
6	0.1903	0.4040	0.2988	0.4842	131.05	40.13	28.07	18.26	pgsD-677	Yes
7	0.2736	0.4270	0.3256	0.5583	199.08	126.49	20.47	21.88	pgsB-618	Yes
8	0.3703	0.4144	0.3006	0.4444	39.04	21.31	59.84	147.05	pgsA-745	Yes
9	0.2398	0.4198	0.2967	0.5245	160.71	77.48	12.56	8.10	pgsD-677	Yes
10	0.4382	0.3447	0.3140	0.4406	100.72	80.86	136.06	242.33	pgsA-745	Yes
11	0.2227	0.4200	0.2901	0.5180	161.08	72.88	15.49	5.54	pgsD-677	Yes
12	0.3396	0.3814	0.2652	0.4321	62.33	15.47	71.34	137.73	pgsA-745	Yes
13	0.2982	0.4305	0.3509	0.5734	214.02	152.83	29.33	39.78	pgsB-618	Yes
14	0.3333	0.5106	0.3443	0.3876	22.19	63.42	162.24	287.35	CHO-K1	Yes
15	0.2985	0.4167	0.3171	0.5522	185.77	116.20	19.02	30.12	pgsB-618	Yes
16	0.3088	0.4270	0.3208	0.5350	140.23	84.72	8.01	34.07	pgsB-618	Yes
17	0.2721	0.4177	0.2703	0.5390	190.19	103.54	19.10	16.30	pgsD-677	Yes
18	0.3568	0.4025	0.2537	0.4402	57.24	18.18	60.12	132.19	pgsA-745	Yes
19	0.2064	0.4548	0.3389	0.5406	177.38	105.12	17.58	6.70	pgsD-677	No
20	0.2034	0.4347	0.3449	0.5449	192.49	111.50	21.97	4.93	pgsD-677	Yes
21	0.3401	0.5006	0.3441	0.4240	9.52	36.83	91.37	200.76	CHO-K1	Yes
22	0.1964	0.4206	0.2975	0.4966	137.31	50.47	20.28	10.46	pgsD-677	Yes
23	0.2076	0.4634	0.3468	0.5475	185.24	116.84	20.03	9.74	pgsD-677	Yes

24	0.3158	0.4747	0.3610	0.4290	6.54	19.13	72.09	166.80	CHO-K1	Yes
25	0.3315	0.3557	0.3307	0.4622	84.98	34.54	61.03	117.52	pgsA-745	Yes
26	0.3141	0.4807	0.3953	0.4432	4.28	24.15	60.91	156.16	CHO-K1	Yes
27	0.3593	0.3661	0.3011	0.4623	81.52	35.10	58.02	122.71	pgsA-745	Yes
28	0.3237	0.4818	0.4029	0.4247	1.06	32.66	93.20	202.66	CHO-K1	Yes
29	0.3529	0.4887	0.3842	0.4226	3.00	41.60	102.76	223.42	CHO-K1	Yes
30	0.2143	0.4098	0.3216	0.4650	83.63	15.43	28.69	43.36	pgsA-745	No
31	0.3926	0.3576	0.3332	0.4123	69.93	56.17	146.12	252.18	pgsA-745	Yes
32	0.2854	0.4284	0.3202	0.5150	110.75	55.02	3.02	28.46	pgsB-618	Yes

Table S13. Identification of the blinded unknowns from the human cell lines using the FRET sensor. LDA was performed on the fluorescence responses of the training set and the unknowns at the same time, and the Mahalanobis distance of each unknown from the centroid of training groups was calculated. The training set included all the five human cell types. Based on the shortest Mahalanobis distance (data that are green colored) from a training group, an unknown is assigned to that particular group. Wrong identifications are red colored. Distance from the groups: d(1) = HeLa; d(2) = HepG2; d(3) = MCF7; d(4) = NT2; d(5) = MCF10A.

Unknown sample #	*FR*				(Mahalanobis distance)^2					Predicted as	Accuracy of identification
	P1	P2	P3	P4	d(1)	d(2)	d(3)	d(4)	d(5)		
1	0.2584	0.4859	0.3472	0.5512	40.80	223.05	146.18	504.81	253.25	HeLa	Yes
2	0.2195	0.5085	0.2290	0.4085	122.52	80.43	61.11	70.73	102.20	MCF7	No
3	0.2668	0.4660	0.2734	0.5335	20.00	181.69	98.90	405.27	221.01	HeLa	Yes
4	0.2010	0.3844	0.3173	0.4278	164.24	249.51	83.90	202.48	40.62	MCF10A	Yes
5	0.2218	0.4384	0.2913	0.4402	51.90	109.88	9.84	131.99	18.79	MCF7	Yes
6	0.1705	0.4296	0.2782	0.4302	115.65	177.22	20.03	97.53	7.75	MCF10A	Yes
7	0.3322	0.5225	0.2608	0.4276	81.07	30.78	133.83	239.06	215.35	HepG2	Yes
8	0.2396	0.4608	0.2969	0.4282	45.05	65.69	13.90	114.84	24.61	MCF7	Yes
9	0.3480	0.5227	0.2816	0.4172	85.40	17.63	145.03	245.45	212.38	HepG2	Yes
10	0.1922	0.4105	0.3000	0.4317	116.68	190.13	37.48	143.30	14.28	MCF10A	Yes
11	0.2696	0.4923	0.2470	0.5345	45.10	186.87	130.23	419.83	277.94	HeLa	Yes

12	0.1762	0.4017	0.2620	0.4397	126.70	218.81	33.14	135.54	26.79	MCF10A	Yes
13	0.2214	0.5123	0.2224	0.4006	142.84	85.51	76.09	67.26	115.83	NT2	Yes
14	0.3043	0.5132	0.2906	0.4188	58.34	11.56	83.82	174.45	131.09	HepG2	Yes
15	0.2106	0.5060	0.2212	0.3504	249.20	125.76	128.67	19.60	120.46	NT2	Yes
16	0.2500	0.4338	0.2866	0.4370	42.57	91.48	17.77	146.41	32.76	MCF7	Yes
17	0.2497	0.4385	0.3183	0.4474	37.55	101.11	27.99	187.27	38.27	MCF7	Yes
18	0.3080	0.5028	0.2490	0.4165	71.37	23.88	87.89	163.10	150.18	HepG2	Yes
19	0.2014	0.5019	0.2195	0.3703	209.34	119.94	97.24	23.23	102.24	NT2	Yes
20	0.2442	0.4478	0.2962	0.4491	26.92	85.96	13.54	161.54	38.23	MCF7	Yes
21	0.1984	0.4983	0.2639	0.3990	126.22	85.84	42.84	41.87	48.20	NT2	Yes
22	0.2687	0.4759	0.2955	0.5638	47.38	247.78	160.29	531.18	302.08	HeLa	Yes
23	0.1957	0.4665	0.3339	0.4352	77.78	119.25	25.96	133.07	13.86	MCF10A	No
24	0.1894	0.4063	0.2802	0.4425	105.73	196.77	29.16	148.28	22.17	MCF10A	Yes
25	0.2008	0.4006	0.3083	0.4405	115.26	207.02	48.89	182.57	27.52	MCF10A	Yes
26	0.2829	0.4828	0.3044	0.5300	18.49	161.97	116.83	429.81	232.76	HeLa	Yes
27	0.2437	0.4860	0.2171	0.4450	63.85	83.40	44.56	139.36	120.30	MCF7	No
28	0.2733	0.4833	0.3009	0.5290	15.89	159.67	105.44	410.52	219.58	HeLa	Yes
29	0.3207	0.5218	0.2668	0.4210	77.91	21.98	116.66	206.43	185.87	HepG2	Yes
30	0.3281	0.5155	0.2974	0.4049	78.23	4.10	112.12	188.52	152.38	HepG2	Yes

References

1. Miranda, O. R.; You, C. C.; Phillips, R.; Kim, I. B.; Ghosh, P. S.; Bunz, U. H. F.; Rotello, V. M. *J. Am. Chem. Soc.* **2007**, *129*, 9856.
2. Kim, I. B.; Dunkhorst, A.; Gilbert, J.; Bunz, U. H. F. *Macromolecules* **2005**, *38*, 4560.
3. You, C. C.; Miranda, O. R.; Gider, B.; Ghosh, P. S.; Kim, I. B.; Erdogan, B.; Krovi, S. A.; Bunz, U. H. F.; Rotello, V. M. *Nat. Nanotechnol.* **2007**, *2*, 318.
4. Kim, I. B.; Phillips, R.; Bunz, U. H. F. *Macromolecules* **2007**, *40*, 5290.
5. Phillips, R. L.; Miranda, O. R.; You, C. C.; Rotello, V. M.; Bunz, U. H. F. *Angew. Chem., Int. Ed.* **2008**, *47*, 2590.
6. Bajaj, A.; Miranda, O. R.; Kim, I.-B.; Phillips, R. L.; Jerry, D. J.; Bunz, U. H. F.; Rotello, V. M. *Proc. Natl. Acad. Sci. U. S. A.* **2009**, *106*, 10912.

7. Medintz, I. L.; Clapp, A. R.; Brunel, F. M.; Tiefenbrunn, T.; Uyeda, H. T.; Chang, E. L.; Deschamps, J. R.; Dawson, P. E.; Mattoussi, H. *Nat. Mater.* **2006**, *5*, 581.

8. (a) Clapp, A. R.; Medintz, I. L.; Mauro, J. M.; Fisher, B. R.; Bawendi, M. G.; Mattoussi, H. *J. Am. Chem. Soc.* **2004**, *126*, 301. (b) K. Boeneman, B. C. Mei, A. M. Dennis, G. Bao, J. R. Deschamps, H. Mattoussi, I. L. Medintz, *J. Am. Chem. Soc.* **2009**, *131*, 3828.

9. Lakowicz, J. R. *Principles of Fluorescence Spectroscopy*, 2nd Edn., Kluwer Academic/Plenum Publishers, New York 1999.

10. Duan, X.; Liu, L.; Feng, X.; Wang, S. *Adv. Mater.* **2010**, *22*, 1602.

11. Phillips, R. L.; Miranda, O. R.; Mortenson, D. E.; Subramani, C.; Rotello, V. M.; Bunz, U. H. F. *Soft Matter* **2009**, *5*, 607.

12. SYSTAT11.0, SystatSoftware, Richmond, CA94804, USA, 2004.

13. Mahalanobis, P. C. *Proc. Natl. Inst. Sci. India* **1936**, *2*, 49.

14. R Development Core Team (2010). *R: A language and environment for statistical computing. R Foundation for Statistical Computing*, Vienna, Austria. ISBN 3-900051-07-0, URL http://www.R-project.org.